Journal of Organometallic Chemistry, 411 (1991) 159–170
Elsevier Sequoia S.A., Lausanne
JOM 21847

Reactions of di- and polynuclear complexes

VIII *. Ligand substitution in $[V_2Cp_2(CO)_4(\mu\text{-SMe})_2]$ by isocyanides or trimethyl phosphite. Synthesis, spectroscopic characterisation of the mono- and di-substituted derivatives. Electrochemical behaviour of the parent complex

François Y. Pétillon, Philippe Schollhammer and Jean Talarmin
URA CNRS No. 322, "Chimie, Electrochimie et Photochimie Moléculaires", Faculté des Sciences, Université de Bretagne Occidentale, 29287 Brest-Cédex (France)

(Received January 16th, 1991)

Abstract

The photo-induced decarbonylation of $[VCp(CO)_4]$ in the presence of an organodisulfide RSSR (R = Ph) or a thiol HSR (R = ^{n}Pr, ^{t}Bu, Et) at room temperature in THF gives the binuclear diamagnetic compounds $[V_2Cp_2(CO)_4(\mu\text{-SR})_2]$ (**1**). Thermal substitution of RNC (R = ^{t}Bu, xylyl) for CO in **1** results in the formation of a mixture of isomeric mono- and di-substituted derivatives $[V_2Cp_2(CO)_3(CNR)(\mu\text{-SMe})_2]$ (**3**) and $[V_2Cp_2(CO)_2(CNR)_2(\mu\text{-SMe})_2]$ (**4**), respectively. The complexes have been characterised by infrared and ^{1}H NMR spectroscopies. The primary reduction of $[V_2Cp_2(CO)_4(\mu\text{-SMe})_2]$ is a partially reversible one-electron step coupled with chemical reactions. The nature of these reactions and of the product of controlled-potential electrolyses are discussed.

Introduction

Intense interest in polynuclear sulfur-rich transition metal complexes in recent years has led to the synthesis and characterisation of a large number of such species [2]. Part of this interest arises from the participation of such species in biological [3], catalytic [4] and hydrodesulfurization [5] processes. Previous reports from this laboratory were concerned with dinuclear thio-bridged molybdenum and tungsten complexes [6]. In contrast to well-investigated sulfur-coordinated complexes of groups 6, 7, and 8 transition metals, relatively little is known about their vanadium relatives [2b,7].

Studies of the chemistry of sulfur-containing vanadium complexes have mainly involved $[VCp(CO)_4]$ as the starting material [7b]. Carbonyl ligands in this com-

---

* For Part VII see ref. 1.

0022-328X/91/$03.50

pound can be photochemically or thermally replaced by one or two Lewis-base type ligands to give mono- or di-substituted complexes [$VCp(CO)_3L$] or [$VCp(CO)_2L_2$] (L = SMe_2 [8], CS [9]). The thermal reactions of the half-sandwich compounds [$VCp(CO)_4$] and [$VCp^\star(CO)_4$] ($Cp^\star = C_5Me_5$) with sulfur or disulfides S_2R_2 in boiling toluene, or with 1,2-ethanedithiol, lead to complete displacement of all CO ligands. In this way a range of [VCp'_2S_4] [10], [VCp'_2S_5] [10,11] (Cp′ = Cp or Cp*), [$V_2Cp_2(\mu\text{-}SR)_4$] (R = Me [12], Ph [13]) and [$V_2Cp_2(\mu\text{-}S_2C_2H_4)_2$] [14] substituted derivatives have been prepared; in all these binuclear complexes there is evidence for a direct metal–metal interaction [15,13]. Several years ago we isolated from the room temperature reaction between [$VCp(CO)_4$] and MeSSMe in THF under UV-light the carbonyl-containing compound [$V_2Cp_2(CO)_4(\mu\text{-}SMe)_2$], an intermediate in the formation of the decarbonylated derivative [$V_2Cp_2(\mu\text{-}SMe)_4$] [16]. On the basis of spectroscopic data we postulated a metal–metal bonded dinuclear structure for this complex; very recently Herberhold et al. [17] confirmed this geometry by an X-ray diffraction study of the related pentamethylcyclopentadienyl vanadium derivative. The formation of such an initial product sheds some light on the mechanism of the decarbonylation of carbonyl-containing vanadium complexes. As an extension of our work in this area, we now describe the formation of new complexes of the type [$V_2Cp_2(CO)_4(\mu\text{-}SR)_2$] (R = Ph, ^{n}Pr, ^{t}Bu, Et) and ligand substitution reactions in [$V_2Cp_2(CO)_4(\mu\text{-}SMe)_2$] with isocyanides and tertiary phosphine. With the aim of gaining information about electron transfer properties of the vanadium complexes we also carried out an electrochemical study of the parent derivative.

Results and discussion

1. Synthetic aspects and spectroscopic characterisation

Photolytic displacement of CO ligands from [$VCp(CO)_4$] in the presence of RSSR (R = Me [16], Ph) in THF gives a mixture of [$V_2Cp_2(CO)_4(\mu - SR)_2$] (R = Me (**1a**), Ph (**1b**)) and the carbonyl-free product [$V_2Cp_2(\mu\text{-}SR)_4$] (**2**). The photo-induced reaction of the tetracarbonylcyclopentadienylvanadium(I) in the presence of HSR (R = Me, ^{n}Pr, ^{t}Bu, Et) leads to the formation of **1** only (**1a**: R = Me; **1c**: R = ^{n}Pr; **1d**: R = ^{t}Bu; **1e**: R = Et).

The ^{1}H NMR spectrum of **1a** shows two sets of singlets of differing intensities for the Cp ring and the methyl protons (Table 1). This is consistent with the presence of a mixture of at least two isomers in solution, as we suggested previously [16]. Two types of isomerism must be considered, involving the relative disposition of the Cp and CO ligands (*cis/trans* isomerism) and/or the mutual orientation of the methyl groups on the bridging S atoms (*syn/anti* isomerism). Our reasons for attributing the *cis–syn* ee and the *cis–anti* geometries to the two isomers in solution are as follows:

(i) The ^{1}H NMR spectrum of **1a** is inconsistent with a *trans* geometry, for which two signals of equal intensities would be expected for the cyclopentadienyl ring protons.

(ii) The gap displacement between the two isomers' ^{1}H NMR resonances (see Table 1) of the two isomers is very small, which is consistent with the small electronic energy differences observed between *syn* and *anti* compared with that between *cis* and *trans* species [18].

Table 1

Spectroscopic data

Complex	IR spectra [a] (cm^{-1})		^1H NMR spectra [b] (ppm)					
	ν(CN)	ν(CO)	S*R* [CH_2 or/and CH_3]	*Me* (RNC)	H_{ring} (RNC or SPh)	Cp	Isomer	Relative abundance (%)
[$V_2Cp_2(CO)_4(\mu\text{-}SMe)_2$] (**1a**)		1985s, 1915s	2.03 (s)			4.65 (s), 4.61 (s)	A (**1a**)	70
			1.99 (s)				B (**1a**)	30
[$V_2Cp_2(CO)_4(\mu\text{-}SPh)_2$] (**1b**)		1995s, 1945m			7.1–7.33 (m)	5.23 (s)		
[$V_2Cp_2(CO)_4(\mu\text{-}S^nPr)_2$] (**1c**)		1990vs, 1930s	0.91 (t) 1.36–1.5 (m) 2.53 (t)			5.06 (s)		
[$V_2Cp_2(CO)_4(\mu\text{-}S^tBu)_2$] (**1d**)		1990s, 1925m	1.36 (s)			5.15 (s)		
[$V_2Cp_2(CO)_4(\mu\text{-}SEt)_2$] (**1e**)		1985vs, 1915s	1.19 (t) 2.57 (q)			5.06 (s)		
[$V_2Cp_2(CO)_3(CN^tBu)(\mu\text{-}SMe)_2$] (**3a**)	2100s, 2060s	1940s, 1895s, 1870sh	2.21 (s), 2.126 (s)	1.07 (s)		4.82 (s), 4.80 (s)	A (**3a**)	55
			2.18 (s), 2.07 (s)	1.05 (s)		4.79 (s), 4.783 (s)	B (**3a**)	24
			2.124 (s), 2.03 (s)	1.07 (s)		4.787 (s)	C(**3a**)	21
[$V_2Cp_2(CO)_2(CN^tBu)_2(\mu\text{-}SMe)_2$] (**4a**)	2100s, 2060sh	1870s, 1850sh	2.27 (s)	1.19 (s)		4.93 (s)	A (**4a**)	50
			2.22 (s)	1.17 (s)		4.92 (s)	B (**4a**)	50
[$V_2Cp_2(CO)_3(CNxylyl)(\mu\text{-}SMe)_2$] (**3b**)	2050s, 1995w	1940s, 1895s, 1870sh	[2.23 (s),	[2.36 (s),		4.84 (s), 4.77 (s)	A (**3b**)	37
			2.21 (s),	2.38 (s),	(6.75)	4.85 (s), 4.78 (s)	B (**3b**)	23
			2.20 (s),	2.39 (s)]		4.83 (s), 4.73 (s)	C (**3b**)	21
			2.18 (s)]			4.82 (s), 4.72 (s)	D (**3b**)	19
[$V_2Cp_2(CO)_2(CNxylyl)_2(\mu\text{-}SMe)_2$] (**4b**)	2040s, 1990m	1895sh, 1865s	2.30 (s), 2.19 (s)	2.44 (s)	7.07	4.94 (s)	A (**4b**)	65
			[2.30 (s), 2.26 (s), 2.22 (s), 2.1 (s), 2.18 (s)]	[2.47 (s), 2.44 (s) 2.43 (s)]	(7.07)	[5.02 (s), 5.00 (s), 4.99 (s), 4.98 (s)]	B–D (**4b**)	35

[a] In CH_2Cl_2 solution. [b] In benzene-d_6 solution, except **4b** in chloroform-*d* solution.

(iii) We assume that the *cis–syn* isomer is a *cis–syn* ee, because: (a) those dinuclear complexes containing a metal of the group 5 of the type $[M_2Cp'_2(CO)_4(\mu\text{-}SR)_2]$ (M = Nb, R = Me, Cp′ = C_5H_5 [19]; M = V, R = Me or Ph, Cp′ = C_5Me_5 [17]) that have been structurally characterised in the solid state all show a *cis–syn* ee geometry; (b) the interactions between the R groups, and between R and Cp would disfavour the *cis–syn* aa geometry [18].

The ^1H NMR spectra of the complexes **1b**–**1e** display a single cyclopentadienyl rings' peak which is indicative of the presence of only one *cis* isomer when R (Ph, ^{n}Pr, ^{t}Bu, Et) is bulky; steric effects can be considered to explain this observation. R ··· R or R ··· Cp interaction considerations, as well as spectroscopic data (Table 1) suggest strongly a *cis–syn* ee geometry for these compounds.

Reaction of $[V_2Cp_2(CO)_4(\mu\text{-}SMe)_2]$ with isocyanides RNC (R = ^{t}Bu, xylyl) and with trimethylphosphite. With the aim of making partially decarbonylated thio-bridged dinuclear vanadium complexes we studied the reaction of **1a** with isocyanides and with trimethylphosphite. The thermal reaction of **1a** with RNC (R = ^{t}Bu, xylyl) in THF gave a mixture of mono- and di-substituted isocyanide derivatives, $[V_2Cp_2(CO)_3(CNR)(\mu\text{-}SMe)_2]$ (R = ^{t}Bu (**3a**), xylyl (**3b**)) and $[V_2Cp_2(CO)_2(CNR)_2(\mu\text{-}SMe)_2]$ (R = ^{t}Bu (**4a**), xylyl (**4b**)), which were separated by column chromatography and isolated as very air-sensitive compounds. The monosubstituted derivatives (**3**) lose CO in the presence of an excess of isocyanide and are converted into compounds **4** (reaction 1).

$$\begin{tikzcd}
{[V_2Cp_2(CO)_4(\mu\text{-}SMe)_2]} \arrow[r, "RNC", "\Delta,\ -CO"'] & {[V_2Cp_2(CO)_3(CNR)(\mu\text{-}SMe)_2]} & + & {[V_2Cp_2(CO)_2(CNR)_2(\mu\text{-}SMe)_2]} \\
\mathbf{(1a)} \arrow[dr, "\Delta", "\text{RNC (excess)}"'] & \mathbf{(3)} \arrow[d, "+RNC"] & & \mathbf{(4)} \\
 & {[V_2Cp_2(CO)_2(CNR)_2(\mu\text{-}SMe)_2]} & & \\
 & \mathbf{(4)} & &
\end{tikzcd} \qquad (1)$$

(R = ^{t}Bu (**a**), xylyl (**b**))

The isocyanide complexes were readily identified spectroscopically and by elemental analysis. Pertinent ^1H NMR and infrared data are listed in Table 1. The complexes **3** are soluble in organic solvents; three bands are observed in the carbonyl stretching region of the infrared spectra (in CH_2Cl_2), in keeping with their formulation. The $\nu(CO)$ absorptions are shifted to lower frequencies relative to those for the parent complex **1a**; this expected lowering reflects the better electron-donor power of the isocyanide ligand compared with that of the carbonyl groups. The presence of two bands in the $\nu(CN)$ region is due to the presence in solution either of two conformers in which the isocyanide ligand has a linear or bent geometry [20] or of *syn*–anti geometrical isomers (see below). The CN stretching bands are shifted toward lower frequencies with increase in the π-acceptor ability of the CNR ligand (Table 1). Upon coordination to vanadium, the $\nu(CN)$ band of the free ligand (R = ^{t}Bu, $\nu(CN) = 2130\ cm^{-1}$; R = xylyl, $\nu(CN) = 2120\ cm^{-1}$) is lowered by 10 to 70 cm^{-1} for ^{t}BuNC and 70 to 130 cm^{-1} for xylylNC. This suggests that electronic effects may be involved and this is consistent with the fact that the aromatic xylyl group provides a better electron delocalisation than aliphatic groups such as t-butyl.

If the absence of *cis* $\rightleftharpoons$ *trans* isomerisation is assumed, the CNR monosubstitution is expected to give three isomers from the mixture of the *cis–anti* and *cis–syn* ee isomers (**1a**) (Scheme 1). Each mono-substituted derivative (**3**) is predicted to have two inequivalent Cp and two inequivalent methyl groups. In practice, the ^{1}H NMR spectrum of **3a** at room temperature is effectively consistent with the presence of one major isomer with inequivalent cyclopentadienyl and methyl groups along with two less-abundant isomers also with inequivalent groups. As these three inseparable isomers have very similar ^{1}H NMR patterns we cannot assign a specific configuration to each of them. Four groups of two singlets are observed at 4.8–4.7 ppm in the ^{1}H NMR spectra of **3b**, which suggests the presence of four isomers when R = xylyl. A *cis–syn* ee $\rightleftharpoons$ *cis–syn* aa isomerisation could be responsible for the number of isomers observed.

There is spectroscopic evidence that complexes **4a** and **4b** are obtained as a mixture of inseparable isomers. Their infrared spectra in the carbonyl stretching region show two bands at lower energy than those for the parent derivative **3**, consistent with disubstitution. For steric and electronic reasons, it seems very likely that the second substitution takes place at the unsubstituted vanadium atom. The result is that there are five possible isomers $\mathbf{4}_{11}$–$\mathbf{4}_{22}$ (Scheme 1) with a non-planar V_2S_2 ring, whose relative stabilities will be determined by Me $\cdots$ Me, Me $\cdots$ C_5H_5, L $\cdots$ C_5H_5 (L = RCN), L $\cdots$ L interactions. The second substitution leads to a new *cis/trans* isomerism related to the position of the isocyanide ligands. Thus, the five isomers have either a L-*cis* ($\mathbf{4}_{11}$–$\mathbf{4}_{13}$) or a L-*trans* ($\mathbf{4}_{21}$–$\mathbf{4}_{22}$) configuration. Every disubstituted isomer **4** is predicted to have a geometry involving equivalent cyclopentadienyl rings and inequivalent methyl groups, except for isomer $\mathbf{4}_{22}$ which has equivalent methyl groups. When L = ^{t}BuNC, only two isomers are observed at room temperature by NMR spectroscopy. We assume that steric hindrance by the ^{t}BuNC ligand disfavours the L-*cis* configuration, and so we assign a L-*trans* geometry to the two isomers detected in the ^{1}H NMR spectrum. When L = xylylNC, five Cp resonances are observed in the ^{1}H NMR spectrum; in this case, the five possible isomers of Scheme 1 may be present. The structure $\mathbf{4}_{13}$ is attributed to the major isomer (65%), which has two inequivalent methylthio-bridged groups and two equivalent Cp rings. The existence in solution of L-*cis* derivatives reflects the smaller steric hindrance by the xylylNC than by the ^{t}BuNC ligand.

Attempts were made to extend the reaction to the synthesis of complexes with a group 15 donor ligand, viz. $[V_2Cp_2(CO)_{4-n}(PR_3)_n(\mu\text{-SMe})_2]$. Surprisingly, neither thermal nor photochemical reaction of $P(OMe)_3$ with **1a** in THF occurred when the reaction was carried out in the presence of catalysts (Me_3NO, PdO), again the expected new complexes were not formed. Finally, direct reaction between $[VCp(CO)_3\{P(OMe)_3\}]$ and HSMe gave only $[V_2Cp_2(CO)_4(\mu\text{-SMe})_2]$.

A limited number of mononuclear vanadium isocyanide complexes have been reported [21], but to our knowledge the complexes described here are the first examples of dinuclear vanadium isocyanide species formed by direct thermal reaction between a dinuclear derivative and RNC. The mononuclear compounds $[VCp(CO)_{4-n}(CNR)_n]$ (n = 1, 2) were made previously by Coville et al. [21] by refluxing a mixture of $[VCp(CO)_4]$ and RNC in toluene, but a metal catalyst was required to bring about CO replacement by RNC. We have known that substitution

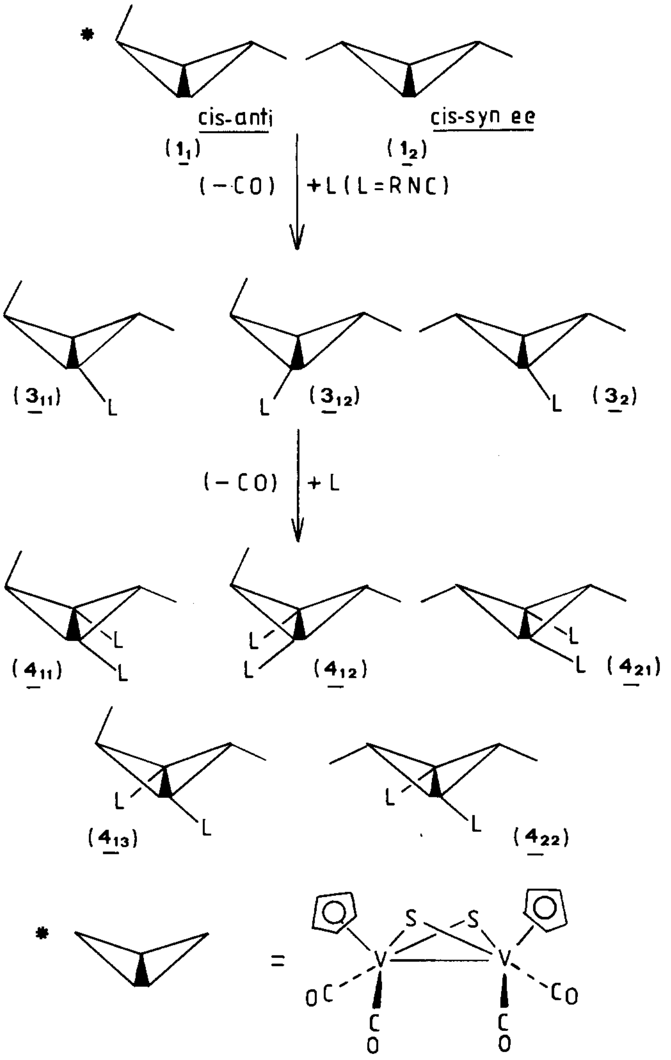

Scheme 1

of RNC for CO in **1a** readily gives rise to divanadium isocyanide derivatives. This contrasts with the results obtained with the analogous molybdenum complex $[Mo_2Cp_2(CO)_4(\mu\text{-SMe})_2]^{2+}$: in that case substitution of RNC for CO could not be brought about thermally, and the synthesis of the substituted derivatives $[Mo_2Cp_2(CO)_{4-n}({}^tBuNC)_n(\mu\text{-SMe})_2]^{2+}$ ($n = 1, 2$) required electrochemical activation [6e]. The replacement of CO by RNC results in an increase in the electron density at the vanadium atoms, and it should be possible to exploit this in new reactions with oxidizing reagents. In view to obtain more information on the electronic properties of dinuclear vanadium complexes we decided to investigate the electrochemical reduction of the parent complex **1a**.

Table 2

Redox potentials of $[V_2Cp_2(CO)_4(\mu\text{-SR})_2]$ in non-aqueous media [a]

R	Solvent	$E^{1/2}_{red1}$ (V/Fc)	Ep_{red2} (V/Fc)	$E^{1/2}_{red3}$ (V/Fc)	$E^{1/2}_{red1}$ (V/Fc)
Me	THF	−2.01 [b]	−2.30 [b]	−2.80 [b]	−0.20 [b]
	MeCN	−1.91 [c]	−2.15 [c]	−2.62 [c]	−0.21 [c]
	CH_2Cl_2	−2.10	−2.32	-	−0.19
Et	THF	−2.04			
Ph	THF	−1.89 [d]			

[a] Cyclic voltammetry data obtained at room temperature unless stated otherwise, $v = 0.2\ V\cdot s^{-1}$. [b] $T = -17\,°C$. [c] $T = -20\,°C$. [d] Peak potential.

2. *Reductive electrochemistry of $[V_2Cp_2(CO)_4(\mu\text{-SMe})_2]$*

The cyclic voltammogram (CV) [22] of $[V_2Cp_2(CO)_4(\mu\text{-SMe})_2]$ (**1a**) in a THF-$[Bu_4N][PF_6]$ electrolyte displays three reduction steps (Table 2). The values of the first reduction potentials of the -SPh and -SEt analogous, shown in Table 2 for comparison, show that this step is affected by the nature of R, the phenylthiolate derivative being, as expected, easier to reduce than its alkylthiolate congeners.

The primary reduction. The increase in the ratio of the anodic to the cathodic peak current, $[(ip^a/ip^c)_{red1}]$, for the primary reduction of $[V_2Cp_2(CO)_4(\mu\text{-SMe})_2]$ from 0.4 at 0.02 Vs^{-1} to 0.47 at 0.2 Vs^{-1} and 0.76 at 1 Vs^{-1} indicates that a chemical reaction is coupled with the electron transfer at Ep_{red1}. The current function $ip^c_{red1}/v^{1/2}$ for this step deviates markedly from linearity at slow scan rates ($v < 0.25\ Vs^{-1}$), suggesting that the reduction at Ep_{red1} occurs by an ECE or an EDisp mechanism [22,23]. The effect of the chemical reaction, which is suppressed by increase in v, is also partially eliminated on lowering the temperature, as illustrated by the CV in Fig. 1 ($T = -17\,°C$): under these conditions, the chemical reversibility of the primary reduction is improved, $(ip^a/ip^c)_{red1} = 0.7$ at 0.2 Vs^{-1}.

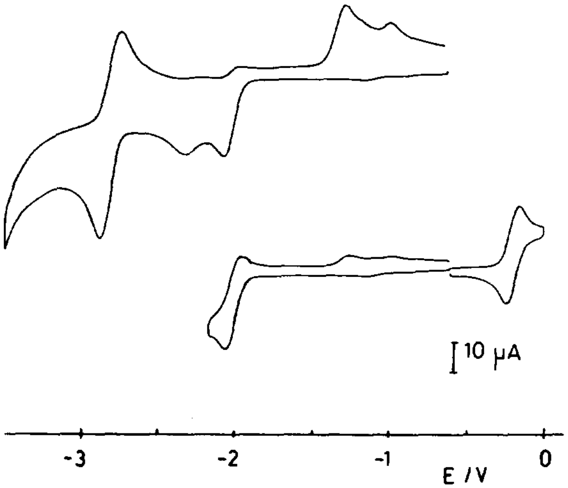

Fig. 1. Cyclic voltammogram of a 0.9 m*M* solution of $[V_2Cp_2(CO)_4(\mu\text{-SMe})_2]$ at −17 °C in THF 0.2 *M* $[Bu_4N][PF_6]$ (vitreous carbon electrode, $v = 0.2\ V\cdot s^{-1}$).

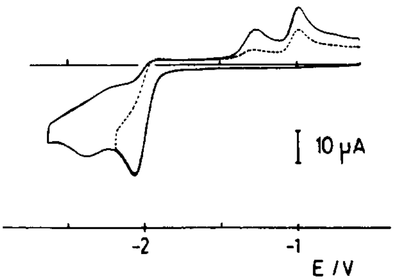

Fig. 2. Cyclic voltammogram of a 1.0 mM solution of $[V_2Cp_2(CO)_4(\mu\text{-SMe})_2]$ in a THF–$[Bu_4N][PF_6]$ electrolyte at room temperature (vitreous carbon electrode, $v = 0.2$ V·s^{-1}).

Comparison of ip^{c}_{red1} with ip^{a}_{ox1} [22*,24*] shows that the primary step of the reduction at Ep_{red1} involves the transfer of a single electron (reaction 2).

$$[V_2Cp_2(CO)_4(\mu\text{-SMe})_2] \underset{\pm 1e}{\rightleftharpoons} [V_2Cp_2(CO)_4(\mu\text{-SMe})_2]^{\dot{-}} \tag{2}$$

The nature of the chemical step coupled with the electron transfer at Ep_{red1} is discussed in more detail later.

The second reduction step. The second cathodic process, characterised by the small, broad peak observed at −2.3 V (Fig. 1), is assigned to a further electronation of $[V_2Cp_2(CO)_4(\mu\text{-SMe})_2]^{\dot{-}}$ (reaction 3). The ratio of the peak currents for the first two reduction processes, $ip^{c}_{red2}/ip^{c}_{red1}$, increases with increasing v and/or on lowering of the temperature, changes which were shown above to make the primary reduction more reversible. Under the conditions used for this study, i.e. $T \geqslant -17\,^\circ$C (THF); $-25\,^\circ$C (MeCN); $v \leqslant 1$ Vs^{-1}, the second step remains irreversible, showing that the dianion undergoes a fast decomposition (reaction 3).

$$[V_2Cp_2(CO)_4(\mu\text{-SMe})_2]^{\dot{-}} + 1e \xrightarrow[-2.30V]{} [V_2Cp_2(CO)_4(SMe)_2]^{2-} \longrightarrow \text{products} \tag{3}$$

Owing to the complete chemical irreversibility of the second electron transfer step, the third, reversible, cathodic process at −2.8 V appears to be due to the reduction of a product generated at either Ep_{red1} or Ep_{red2}.

The reduction mechanism of $[V_2Cp_2(CO)_4(\mu\text{-SMe})_2]$. We have shown that the reduction at Ep_{red1} occurs by an ECE or an EDisp mechanism on the CV time scale. That the reductions at Ep_{red1} and Ep_{red2} both lead to the same products (Fig. 2) strongly suggests that the chemical step coupled with the electron transfer at Ep_{red1} is the disproportionation of $[V_2Cp_2(CO)_4(\mu\text{-SMe})_2]^{\dot{-}}$, followed by the fast decomposition of the dianion (Scheme 2). The overall reduction at Ep_{red1} and Ep_{red2} can be represented by reaction 4.

$$[V_2Cp_2(CO)_4(\mu\text{-SMe})_2] + 2e \longrightarrow \text{products} \tag{4}$$

However, exhaustive controlled-potential electrolyses carried out at Ep_{red1} or Ep_{red2} require less than 2F/mol of starting material ($n \sim 1.5$ F/mol). The CV of the catholyte shows the oxidation peak at −1.0 V, whereas the reversible reduction at −2.8 V and the irreversible oxidation at −1.3 V are absent. These two processes are

---

* Reference number with asterisk indicates a note in the list of references.

$$[V_2Cp_2(CO)_4(\mu\text{-}SMe)_2] \underset{+1\,e^-}{\rightleftharpoons} [V_2Cp_2(CO)_4(\mu\text{-}SMe)_2]^{\dot{-}} \qquad E^\circ_{red1}$$

$$2[V_2Cp_2(CO)_4(\mu\text{-}SMe)_2]^{\dot{-}} \rightleftharpoons [V_2Cp_2(CO)_4(\mu\text{-}SMe)_2] + [V_2Cp_2(CO)_4(SMe)_2]^{2-}$$

$$[V_2Cp_2(CO)_4(SMe)_2]^{2-} \longrightarrow \{[V_2Cp_2(CO)_4(\mu\text{-}SMe)]^-\} + SMe^-$$

$$[V_2Cp_2(CO)_4(\mu\text{-}SMe)_2] + SMe^- \longrightarrow \{[V_2Cp_2(CO)_4(\mu\text{-}SMe)]^-\} + MeSSMe$$

Scheme 2. Mechanism of reduction of $[V_2Cp_2(CO)_4(\mu\text{-}SMe)_2]$ at Ep_{red1}.

therefore assigned to an unstable intermediate in the reduction. A plot of the cell current against charge passed is linear at the beginning of the electrolysis, with a slope indicating the consumption of 2F/mol of complex, and then falls more rapidly than expected from the first part of the curve. This behaviour shows that after an induction period the electroactive material is consumed in a non-electrochemical path. The new chemical reaction (not detected by CV) involves $[V_2Cp_2(CO)_4(\mu\text{-}SMe)_2]$ and a product generated by its reduction. A potential reducing agent is the anion SMe^-, which could result from the decomposition of $[V_2Cp_2(CO)_4(SMe)_2]^{2-}$. Addition of $[Et_4N][SMe]$ to a solution of $[V_2Cp_2(CO)_4(\mu\text{-}SMe)_2]$ did, indeed, result in marked suppression of the primary reduction peak current and resulted in the formation of the same species as that observed after electrolysis ($Ep_{ox} = -1.0$ V).

The metal complex arising from the decomposition of $[V_2Cp_2(CO)_4(SMe)_2]^{2-}$ and from the reaction of the thiolate anion with the parent neutral complex is shown between parentheses in Scheme 2. Its nature could not be ascertained because we were unable to separate the product of the electrolysis from the supporting electrolyte. Nevertheless, the proposed formulation, e.g. $[V_2Cp_2(CO)_4(\mu\text{-}SMe)]^-$ (a V=V double bond is required for the metal centres to achieve an 18-electron configuration), is consistent with all the electrochemical observations.

In the molybdenum complex $[Mo_2Cp_2(CO)_4(\mu\text{-}SH)_2]^{2+}$, which is isostructural [6d,17] and isoelectronic with $[V_2Cp_2(CO)_4(\mu\text{-}SMe)_2]$, the π^*(Mo–Mo) LUMO is separated by only ca 0.2 eV from a metal–metal bonding [π(Mo–Mo)] orbital possessing an antibonding contribution of the bridging SH groups [18]. Inversion of these closely spaced levels may be envisaged in the vanadium complex, owing to slightly different structural parameters such as the M–M separation and the dihedral angle between the two M–S–M wings. In such a situation the population of the LUMO of $[V_2Cp_2(CO)_4(\mu\text{-}SMe)_2]$ would result in the strengthening of the V–V interaction and in weaker V–S bonds. This is wholly consistent with the formulation we propose for the reduction product, e.g. $[V_2Cp_2(CO)_4(\mu\text{-}SMe)]^-$ (V=V).

The reductive behaviour of $[V_2Cp_2(CO)_4(\mu\text{-}SMe)_2]$ reported here is markedly different from that of $[Mo_2Cp_2(CO)_4(\mu\text{-}SMe)_2]^{2+}$ [6d]. The vanadium complex is much harder to reduce than the molybdenum dication ($\Delta E^{1/2}_{red} \sim 1.5$ V) and the reduction mechanism and products are quite different. The large potential separation between the reduction of the two complexes can be attributed, at least in part, to the dipositive charge carried by the molybdenum compound. The origin of the difference in the reduction mechanism (and in the reduction products) for the two complexes [25*] may lie in the different nature of the LUMO's of the vanadium and of the molybdenum species.

Experimental

The reactions were performed under nitrogen or argon by standard Schlenk techniques and in solvents deoxygenated and dried by standard methods. Infrared spectra were recorded on a Pye-Unicam SP 2000 spectrophotometer in dichloromethane solutions. NMR spectra (^1H) in C_6D_6 or $CDCl_3$ solutions, were recorded on a JEOL FX 100 or a Bruker AC 300 with Me_4Si as reference. Chemical analyses were performed by the "Centre de Microanalyses du CNRS de Lyon".

The complex $[V_2Cp_2(CO)_4(\mu\text{-}SMe)_2]$ was prepared by the published method [16]. All other reagents were commercial grade and used as obtained.

For the photo-induced CO eliminations a Hanau TQ 150 mercury vapour lamp was used.

Electrochemistry

The electrochemical equipment (apparatus, cells, set of electrodes) was as described previously [6d]. Ferrocene was added as an internal standard at the end of the experiments and the potentials (text, table, figures) are referenced to the ferrocene/ferrocenium ion couple.

General procedure for the preparation of $[V_2Cp_2(CO)_4(\mu\text{-}SR)_2]$ (1)

*(a) Synthesis of $[V_2Cp_2(CO)_4(\mu\text{-}SPh)_2]$ (**1b**).* **1b** was prepared by the procedure described previously for **1a** [16]. The product was purified by chromatography on silica, the dinuclear complex **1b** was eluted with hexane/CH_2Cl_2 (1/5).

1b (R = Ph): Red solid, yield 60%. Anal. Found: C, 56.2; H, 3.9; S, 11.5; V, 17.2. $C_{26}H_{20}O_4S_2V_2$ calcd.: C, 55.6; H, 3.6; S, 11.4; V, 18.1%.

*(b) Synthesis of $[V_2Cp_2(CO)_4(\mu\text{-}SR)_2]$ ($R = {}^nPr$ (**1c**), ${}^tBu$ (**1d**), Et (**1e**)).* In a typical preparation a solution of $[VCp(CO)_4]$ (3.5 mmol in 30 cm^3 THF) was added to a slight excess of thiol (ca 3.7 mmol in 20 cm^3 THF). The mixture was stirred and irradiated for 24 h and then evaporated to dryness. After extraction with dichloromethane, the extract was chromatographed on a silica gel column, with hexane/CH_2Cl_2 (1/5) as eluent, to give complexes **1c–e**, which were recrystallised from hexane/CH_2Cl_2.

1c ($R = {}^nPr$): Blood-red solid, yield 38%. Anal. Found: C, 48.6; H, 4.6; S, 13.1; V, 20.6. $C_{20}H_{24}O_4S_2V_2$ calcd.: C, 48.9; H, 4.1; S, 13.1; V, 20.7%.

1d ($R = {}^tBu$): Blood-red solid, yield 8%. Anal. Found: C, 50.1; V, 18.9. $C_{22}H_{28}O_4S_2V_2$ calcd.: C, 50.5; V, 19.5%.

1e (R = Et): Blood-red solid, yield 55%. Anal. FOund: C, 46.3; H, 4.3; S, 13.1. $C_{18}H_{20}O_4S_2V_2$ calcd.: C, 46.3; H, 4.3; S, 13.7%.

Preparation of the complexes $[V_2Cp_2(CO)_{4-n}(CNR)_n(\mu\text{-}SMe)_2]$ (n = 1 (3), n = 2 (4))

In a typical procedure, to a solution of ca 0.15 g of $[V_2Cp_2(CO)_4(\mu\text{-}SMe)_2]$ (0.35 mmol) in THF (30 ml) under nitrogen was added a THF solution of the isocyanide (ca 0.5 mmol). The mixture was heated with stirring at 30–40 °C for 1 h. The resulting purple-red solution was then evaporated and chromatographed on a silica gel column. Elution with pentane/CH_2Cl_2 (2:1) gave a red band, which yielded complex **3**. Further elution with CH_2Cl_2 afforded a red fraction of **4**.

3a ($R = {}^tBu$): Red-brown solid, yield 12%. Anal. Found: V, 20.9; N, 2.2. $C_{20}H_{25}NO_3S_2V_2$ calcd.: V, 20.6; N, 2.8%.

3b (R = xylyl): Brown solid, yield 56%.

4a (R = ^{t}Bu): Brown solid, yield 55%. Anal. Found: V, 18.8; N, 2.7. $C_{24}H_{25}NO_3S_2V_2$ calcd: V, 18.8; N, 2.6%.

4b (R = xylyl): Brown solid, yield 30%. Anal. Found: V, 16.9; N, 4.3; C, 58.6. $C_{32}H_{34}N_2O_2S_2V_2$ calcd.: V, 15.8; N, 4.3; C, 59.6%.

Acknowledgements

The CNRS (Centre National de la Recherche Scientifique) is thanked for financial support. The authors are grateful to Dr. R. Pichon for assistance with the NMR experiments.

References and notes

1 R. Rumin, F. Robin, F.Y. Pétillon, K.W. Muir and I. Stevenson, Organometallics, in press.

2 (a) P.J. Blower and J.R. Dilworth, Coord. Chem. Rev., 76 (1987) 121; (b) J. Wachter, Angew. Chem., Int. Ed. Engl., 28 (1989) 1613.

3 (a) S.D. Conradson, B.K. Burgess, W.E. Newton, L.E. Mortenson and K.O. Hodgson, J. Am. Chem. Soc., 109 (1987) 7507; (b) S.J.N. Burgmayer and E.I. Stiefel, J. Chem. Educ., 62 (1985) 943; (c) B. Hedman, P. Franck, S.F. Gheller, L. Roe, W.E. Newton and K.O. Hodgson, J. Am. Chem. Soc., 110 (1988) 3798.

4 R.R. Chianelli, Catal. Rev.-Sci. Eng., 26 (1984) 361; (b) M. Rakowski DuBois, Chem. Rev., 89 (1989) 1.

5 (a) W. Eltzner, M. Breysse, M. Lacroix, C. Lequlerq, M. Vrinat, A. Müller and E. Dieman, Polyhedron, 7 (1988) 2405; (b) M. Rakowski DuBois, J. Am. Chem. Soc., 105 (1983) 3710; (c) F.E. Massoth, Adv. Catal., 27 (1978) 265.

6 See for example: (a) F.Y. Pétillon, J.L. Le Quéré, J. Roué, J.E. Guerchais and D.W.A. Sharp, J. Organomet. Chem., 204 (1981) 207; (b) J.L. Le Quéré, F.Y. Pétillon, J.E. Guerchais, Lj. Manojlović-Muir, K.W. Muir and D.W.A. Sharp, ibid., 249 (1983) 127; (c) M.B. Gomes de Lima, J.E. Guerchais, R. Mercier and F.Y. Pétillon, Organometallics, 5 (1986) 1952; (d) J. Courtot-Coupez, M. Guéguen, J.E. Guerchais, F.Y. Pétillon, J. Talarmin and R. Mercier, J. Organomet. Chem., 312 (1986) 81; (e) M. El Khalifa, M. Guéguen, R. Mercier, F.Y. Pétillon, J.Y. Saillard and J. Talarmin, Organometallics, 8 (1988) 140; (f) M. Guéguen, F.Y. Pétillon and J. Talarmin, Organometallics, 8 (1988) 148.

7 (a) L. Messerle, Chem. Rev., 88 (1988) 1229; (b) S.C. Srivastava and A.K. Shrimal, Polyhedron, 7 (1988) 1639.

8 A. Belforte, F. Calderazzo and P.F. Zanazzi, Gazz. Chim. Ital., 115 (1985) 71.

9 S. Rajan, Indian J. Chem., Sect. A, 15 (1977) 920.

10 M. Herberhold and Kuhnlein, New. J. Chem., 12 (1988) 357.

11 R.A. Schunn, C.J. Fritchie, Jr. and C.T. Prewitt, Inorg. Chem., 5 (1966) 892.

12 R.H. Holm, R.B. King and F.G.A. Stone, Inorg. Chem., 2 (1963) 219.

13 A.A. Pasynskii, I.L. Eremenko, B. Orazsakhatov, Y.V. Rakitin, V.M. Novotortsev, O.G. Ellert and V.T. Kalinnikov, Inorg. Chim. Acta., 39 (1980) 91.

14 O.A. Rajan, M. McKenna, J. Noordik, R.C. Haltiwanger and M. Rakowski DuBois, Organometallics, 3 (1984) 831.

15 C.M. Bolinger, T.B. Rauchfuss and A.L. Rheingold, J. Am. Chem. Soc., 105 (1983) 6321.

16 F.Y. Pétillon, J.L. Le Quéré and J.E. Guerchais, Inorg. Chim. Acta, 37 (1979) L453.

17 M. Herberhold, M. Kuhnlein, W. Kremnitz and A.L. Rheingold, J. Organomet. Chem., 383 (1990) 71.

18 M. El Kalifa, F.Y. Pétillon, J.Y. Saillard and J. Talarmin, Inorg. Chem., 28 (1989) 3849.

19 W.A. Herrmann, H. Biersack, M.L. Ziegler and B. Balbach, J. Organomet. Chem., 206 (1981) C33.

20 (a) G.W. Harris, M.O. Albers, J.C.A. Boeyens and N.J. Coville, Organometallics, 2 (1983) 609; (b) P.D. Harvey, I.S. Butler, G.W. Harris and N.J. Coville, Inorg. Chem., 25 (1986) 3608.

21 N.J. Coville, G.W. Harris and D. Rehder, J. Organomet. Chem., 293 (1985) 365, and references therein.

22 Abbreviations used: CV: cyclic voltammetry; ip^a: anodic peak current; ip^c: cathodic peak current; Ep: Peak potential; $E^{1/2} = (Ep^a + Ep^c)/2$; $\Delta Ep = Ep^a - Ep^c$; v: scan rate; n: number of electrons. An ECE process involves sequential electron transfer (E) and chemical (C) steps. An ECDisp process comprises an electron transfer followed by the disproportionation of the electrogenerated species.

23 A.J. Bard and L.R. Faulkner, Electrochemical Methods. Fundamentals and Applications, Wiley, New York, 1980.

24 Although the oxidation of the complex was not investigated in detail, the first anodic step is shown in Fig. 1 since it appears as a reversible one-electron process [23] at −17 °C: $(ip^c/ip^a)_{ox1} = 1$; $\Delta Ep = 80$ mV (THF-electrolyte); $\Delta Ep = 60$ mV (MeCN-electrolyte).

25 The molybdenum dication undergoes a single step 2 electron reduction reversible on the CV time scale, followed by isomerisation [6d].